



## Development of Fault Detection, Isolation Strategy, and Robust Fault Tolerant Controller to Sustain Flight Control System Accurate Failures

**Nagarathna K<sup>\*1</sup>, Girish S.Deodhare<sup>\*2</sup>**

<sup>\*1</sup>Research Scholar, Aeronautical Development Agency, VTU-Research Center, Associate Professor, Global Academy of Technology, Bengaluru-560098, India

<sup>\*2</sup> Distinguished Scientist, Director General –ADA and Programme Director Development Agency, Vimanapura Post , Bengaluru-560017, India

**Abstract:-** In this article study, a Fault Detection and Isolation (FDI) algorithm of n-channel redundant Flight Control Computer which compares the inputs received from the sensors on different channels and detects and isolates the faulty channels. The inputs from remaining healthy channels are mediated and forwarded to controller. It further demonstrates the performance of Proportional Integral and Derivative controller in presence of actuator stuck and actuator ineffective faults detected through the FDI algorithm. Also, the robustness of controller has been demonstrated.

**Keywords:** FDI, Fault tolerant, redundancy manager, aircraft, plant, actuators, controllers, robustness, failure.

### 1. Introduction

The safety-critical applications which are automated, like aircraft, requires redundant hardware to facilitate fault recovery and sustain the mission. Such systems have fail-operational capability and are made impervious to any single point component failure. Fail-safe systems make controlled shut-down to a safe state when FTC systems, as an emerging and attractive topic in the field of automatic control, have received more and more attention in recent years. One of the earliest papers in the field of FTC by Stengel [1] published in 1991, investigated the concepts of FTC and importance of artificial intelligence application in FTC systems. The Patton [2] & Luze and Richter [3] reviewed the FTC techniques and analyzed the key issues of FTC design [2]. Faults and failures in the components of a control system can endanger the system stability and degrade its performance. Fault in a dynamical system can be described as a deviation of the system structure or system parameters from a nominal situation [5]. The overall effect of a single fault in a system can be varied from performance degradation to a total failure [4]. It is worthwhile to mention the difference between faults and system uncertainties and external disturbances. The faults are those



elements that should be detected and whose effects should be removed by remedial actions. Disturbances and model uncertainties are nuisances, which are known to exist but whose effects on the system performance are handled by appropriate measures like filtering or robust design. In theory, it has been demonstrated that controllers can be designed to attenuate disturbances and tolerate model uncertainties up to a certain size, while faults are more severe changes, whose effects on the plant behaviour cannot be surpassed by a fixed controller. The difference between faults and failures should also be illustrated. A fault causes a change in the characteristics of a component such that the mode of operation or performance of the component is changed in an undesired way. Hence, the required specifications for the system performance are no longer met. In general, a fault can be “worked around” by fault-tolerant control, so the faulty system remains operational. In contrast to this, the notion of a failure describes the inability of a system or a component to accomplish its function. The system or component has to be shut off because the failure is an irrecoverable event. Therefore, redundancy is the main solution in presence of a failure in the system [5]. In order to determine the fault FDI algorithm plays an important role. The most common technique used in FDI is model based technique where in mathematical model of the system is known a priori. The estimated outputs are compared with the actual outputs in order to determine the fault [6]. Another technique which is commonly used is based on Neural networks as demonstrated by Abbaspour et al [5], where the FDI system detects and isolates the fault without the need of controller reconfiguration.

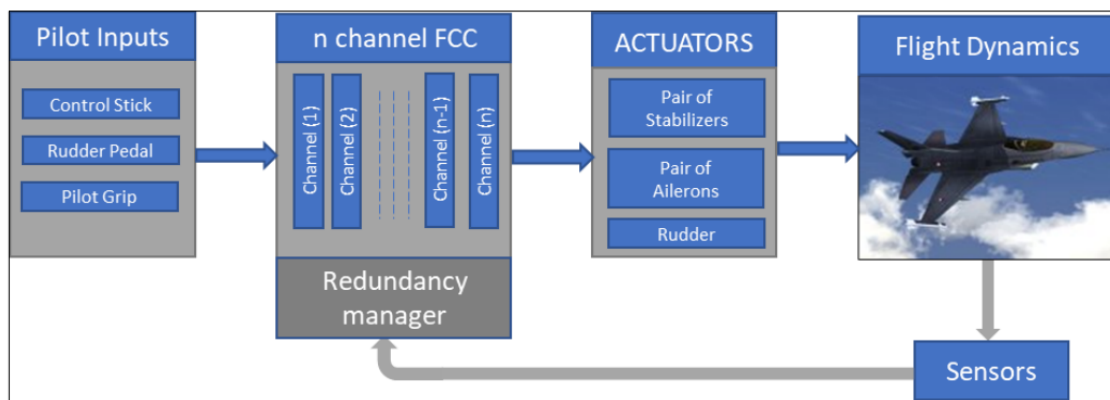


**Fig.1:** Control Architecture with Flight Control Computer & (RM) Redundancy Manager

### 1.1 Targeted Area

This paper shall discuss the Fault Detection and Isolation Algorithm which shall detect and isolate the failures pertaining to sensors and actuators of n-channel redundant Flight



Control System (FCS). Further the paper elaborates on the design and analysis of robust Fault Tolerant Controller which shall sustain the actuator ineffective and actuator stuck faults.

## 2. Fault Detection and Isolation

The FDI algorithm proposed here is based on the precision of  $n$ -inputs received from  $n$ -sensors on  $n$ -different channels by FCC. It is assumed that the Flight control computer have  $n$ -channel ( $n > 2$ ) redundancy. The FCC consist of an RM (redundancy manger) of which compares the inputs of a parameter from  $n$ -different channels up to precision of  $m\%$ , computes the median of the inputs and forwards the median to the controller. If an input from any channel, say channel- $q$ , found out to be deviated by more than  $\pm m\%$ , for a persistency period of  $p$  milliseconds, then the input from channel-  $q$  is ignored and shall be declared failed. In such case the median shall be computed from the other tracking channels. The schematic of a redundancy manager is shown in figure 2.0. It has three stages namely, Input, Voting and Output. The Input stage is responsible for receiving inputs from different sensors and stores them in a buffer. It shall have necessary hardware to do so. The Voting stage is for monitoring the precision of received inputs. It shall compare the inputs from different channels for persistency period  $p$  and shall declare channels input invalid if found deviating by more than  $\pm m\%$ . The Output stage shall receive the voted (valid) inputs from voting stage and compute the median. It shall forward the computed for further processing to controller. The Redundancy Manager shall also monitor the inline and analog health of the sensors on different channels and shall abandon the inputs from a channel if found unhealthy. This paper shall also show the simulation results of two type of faults namely actuator stuck and ineffective (free floating) control surface. The actuators can get stuck and locked to one place or it can become ineffective due to insufficient restraining force leading to free float of control surface. It has been demonstrated that how the control law deals with these issues and ensures safe flight. The plant model used here is of F16 Aircraft and the controller used here is a Proportional Integral and Derivative controller. It has been shown that the controlled surface stuck fault has been detected and isolated appropriately through FDI algorithm as discussed.

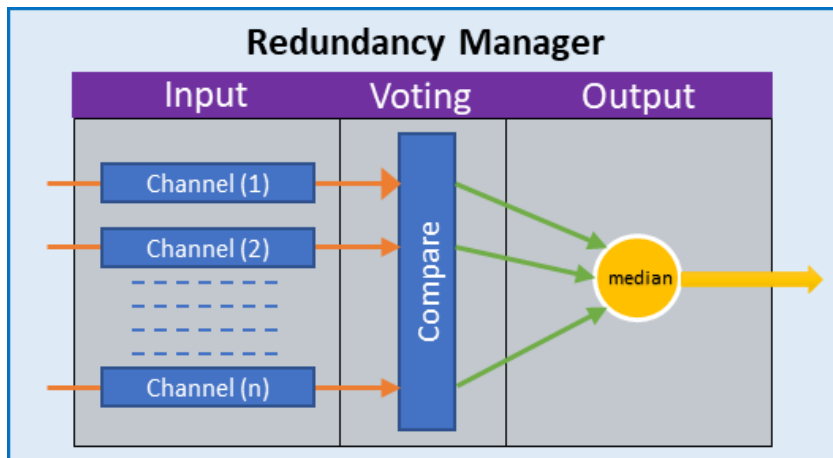


**Fig.2:** Various stages of redundancy manager

## 2.1 Plant Model

Here, the plant is a generic F16 model. The governing *Force* and *Moments* equations are as follows.

$$\sum \vec{Moments} = \frac{d\vec{H}}{dt}$$

$H = \text{angular momentum}$

$$\sum \vec{Force} = m \frac{d\vec{v}}{dt}$$

The Force and moment equations are as follows,

$$F_x = m(u + qw - rv)$$

$$F_y = m(v + ru - pw)$$

$$F_z = m(w + pv - qu)$$

$$L = I_x \dot{q} - I_{zz} \dot{r} + qr(I_z - I_y) - I_{zz} pq$$

$$M = I_y \dot{q} + (I_x - I_z) - I(p^2 - q^2)$$

$$N = I_z \dot{r} - I_{zz} \dot{p} + pq(I_y - I_x) - I_{zz} qr$$

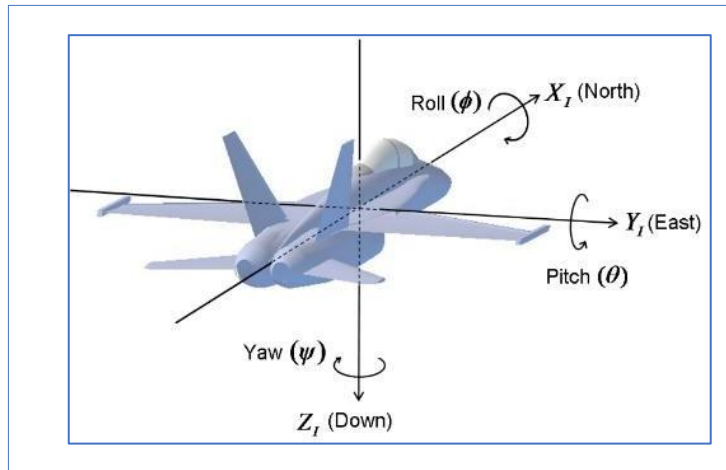


**Fig.3:** Coordinates of the Aircraft axis

**Table.1:** Variable nomenclatures

Paramete <b>r</b>	Description
$X, Y, Z$	Reference aircraft axis
$F_x, F_y$ and $F_z$	Forces along X, Y and Z axis respectively
$L, M$ and $N$	Moments about the X, Y and Z axis respectively
$I_x, I_y$ and $I_z$	moments of inertia about the X, Y and Z axes respectively
$I_{xy}, I_{yz}$ and $I_{xz}$	Cross moments of inertia
$p, q$ and $r$	roll, pitch, yaw rates about X, Y, Z axes respectively
$u, v$ and $w$	airspeed in X, Y, Z axes direction respectively

The actuators are assumed to have time constant of 50 msec. The Simulink® diagram of the completesystem is shown in the Fig.4.

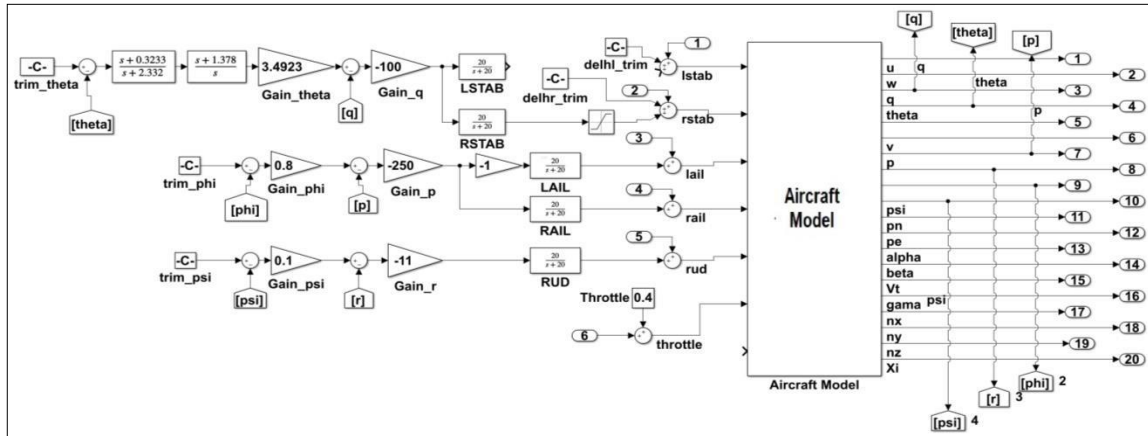


**Fig.4:** Simulink® diagram of Plant with controller

**Table.2:** Trim conditions

Sl. No.	Parameter	Value
1)	$\theta_{trim}$	0.1952 rad
2)	$\phi_{trim}$	0
3)	$\psi_{trim}$	-1.5708 rad
4)	$H_{trim}$	600 m
5)	$p_{trim},$ $q_{trim},$ $r_{trim}$	0
6)	$u_{trim}$	81.3053 m/s
7)	$v_{trim}$	0
8)	$w_{trim}$	16.0794 m/s

### 3. Design Procedure

The design procedure includes the linearization of nonlinear model of aircraft at flight conditions listed in Table 2. The general aircraft model is as follows:



$$\begin{aligned} \dot{u} &= rv - qw - g \sin\theta + \frac{\phi u_x + I}{m \phi C_y} \\ \dot{v} &= pw - ru + g \cos\theta \sin\phi + \frac{m}{\phi C_z} \\ \dot{w} &= qu - pv + g \cos\theta \cos\phi + \frac{m}{m} \\ \dot{p}I_x - \dot{r}I_{xz} &= -\dot{\phi}bC_l - qr(I_z - I_y) + qpl_{xz} \\ \dot{q}I_y - \dot{r}I_{xz} &= -\dot{\phi}C_m - pr(I_x - I_z) - (p^2 - r^2)I_{xz} - rh_{eng} \\ \dot{r}I_z - \dot{p}I_{xz} &= -\dot{\phi}bC_n - pq(I_y - I_x) - qrI_{xz} + qh_{eng} \\ \phi &= p + \tan\theta (q \sin\phi + r \cos\phi) \\ \theta &= q \cos\phi - r \sin\phi \\ \psi &= \frac{q \sin\phi + r \cos\phi}{\cos\theta} \\ \ddot{h} &= u \sin\theta - v \cos\theta \sin\phi - w \cos\theta \cos\phi \end{aligned}$$

Subsequently, the Jacobians are computed as follows;

$$\mathbf{u} = \begin{bmatrix} \delta_{th} \\ \delta_e \\ \delta_a \\ \delta_r \end{bmatrix}$$

$$\begin{aligned} \mathbf{A} &= \begin{bmatrix} \frac{\partial f_1}{\partial x_1} & \dots & \frac{\partial f_1}{\partial x_n} \\ \vdots & \ddots & \vdots \\ \frac{\partial f_n}{\partial x_1} & \dots & \frac{\partial f_n}{\partial x_n} \end{bmatrix} @ \mathbf{x}_0 \\ \mathbf{B} &= \begin{bmatrix} \frac{\partial f_1}{\partial u_1} & \dots & \frac{\partial f_1}{\partial u_m} \\ \vdots & \ddots & \vdots \\ \frac{\partial f_n}{\partial u_1} & \dots & \frac{\partial f_n}{\partial u_m} \end{bmatrix} @ \mathbf{x}_0 \end{aligned}$$

Where  $\mathbf{x} \in \mathbf{R}^n$  is the state vector

$$\mathbf{x} = \begin{bmatrix} u \\ F_{W1} \\ I_q \\ I_\theta \\ I_h \\ \vdots \\ I^p \\ I^r \\ I_\phi \\ [\psi] \end{bmatrix}$$

And  $\mathbf{u} \in \mathbf{R}^m$  is a control vector



**Table.3:** Actuators trim positions

Sl. No.	Control surfaces	Trim values
1.	$\delta_{th}$ (throttle)	18.2 %
2.	$\delta_e$ (elevator)	-0.63°
3.	$\delta_a$ (aileron)	0°
4.	$\delta_r$ (rudder)	0°

**Table.4:** Flight Configurations

Sl. No.	Parameters	Value s
1.	Mass of aircraft	9295 Kg
2.	Chord length	3.45 m
3.	Moment of Inertia	$I_x = 12875;$ $I_y = 75674;$ $I_z = 85552;$ $I_{xz} = 1331;$

And  $\mathbf{x}_0 \in \mathbf{R}^n$  is the vector for initial conditions listed in table 1.0, and  $\mathbf{f} \in \mathbf{R}^p$  is the vector offunctions derived from the differential equations stated in the generic model section.

$$\dot{\mathbf{x}} = \mathbf{f}(\mathbf{x}, \mathbf{u})$$

$$\mathbf{f} = \begin{bmatrix} f_1 \\ f_2 \\ f_3 \\ \vdots \\ f_p \end{bmatrix}$$

The linearized aircraft system can be expressed as follows,

$$\begin{aligned} \dot{\mathbf{x}} &= \mathbf{Ax} + \mathbf{Bu} \\ \mathbf{y} &= \mathbf{Cx} \end{aligned}$$

Here,  $\mathbf{C}$  is the output matrix. The system matrix  $\mathbf{A}$ , input matrix  $\mathbf{B}$  and output matrix  $\mathbf{C}$  are used for deriving the gains of controller for longitudinal, lateral and directional control





Received: 16-01-2024

Revised: 12-02-2024

Accepted: 07-03-2024

$$C = \begin{bmatrix} -0.1319 & 0 & 0 & 0 & 0 & 0 & 0 & 0 & 0 & 0 & 0 \% \text{ alpha} \\ 0.6786 & & & & & & & & & & \\ 0.9816 & 0.190 & 0 & 0 & 0 & 0 & 0 & 0 & 0 & 0 & 0 \% \text{ Vt} \\ & 8 & & & & & & & & & \\ 0 & 0 & 0 & 0 & 0 & 0 & 0.691 & 0 & 0 & 0 & 0 \% \text{ beta} \\ & & & & & & 3 & & & & \\ 0 & 0 & 0 & 0 & 1 & 0 & 0 & 0 & 0 & 0 & 0]; \% \text{ H} \end{bmatrix}$$

$$D = \text{zeros} \\ (4,4);$$

The reduced state matrix A with only longitudinal states  $u, w, q$  and  $\theta$  along with input matrix  $B(\delta_{th}, \delta_e, \delta_a, \delta_r)$  and output matrix  $C(\alpha, V_t)$  are as follows.

$$A = \begin{bmatrix} -0.0213 & 0.1313 & -15.0708 & -9.6298 \\ -0.1192 & -0.6055 & 73.6614 & -1.8717 \\ -0.0001 & 0.001 & -0.6464 & 0 \\ 0 & 0 & 1 & 0]; \end{bmatrix}$$

$$B = \begin{bmatrix} 0.0161 & 7.1522 & 0 & 0 & ; & \% \\ -0.1254 & 0 & 0 & 0 & ; & \% \\ -0.0512 & 0 & 0 & 0 & ; & \% \\ 0 & 0 & 0 & 0 & ]; & \% \end{bmatrix}$$

$$C = \begin{bmatrix} -0.1319 & 0.6786 & 0 & 0 \\ 0.9816 & 0.1908 & 0 & 0]; \end{bmatrix}$$

$$D = \text{zeros} (4, 4);$$

The poles of the system are  $-0.8950, -0.2835, -0.1422$  and  $0.0475$

The dominant pole of the system is  $0.0475$  having damping ratio  $-1.0$ , which is dynamically unstable. Considering the dominant pole, the time to double for this system is  $14.59$  seconds.

#### 4. Simulation and Failure analysis

Extensive simulations were carried out at different flight conditions in normal and failure modes. The results pertaining to two common faults specific to actuators have been analyzed in the following paragraphs.



### 4.1 Actuator Stuck Problem:

The plots representing this problem are shown in figure 5, 6, and 7. The model is subjected to change in the pitch angle  $\theta$ , which results change in position of control surfaces as well changes in the pitchrate  $q$  accordingly. The fault is introduced at around 48 sec in LSTAB (left stabilizer) where it gets stuck at  $5^\circ$  and locked. Subsequently, it can be observed that RSTAB (right stabilizer) pushes itself further down to create sufficient lift and at the same time Ailerons are moved in differential way to counter the moment out of LSTAB stuck.

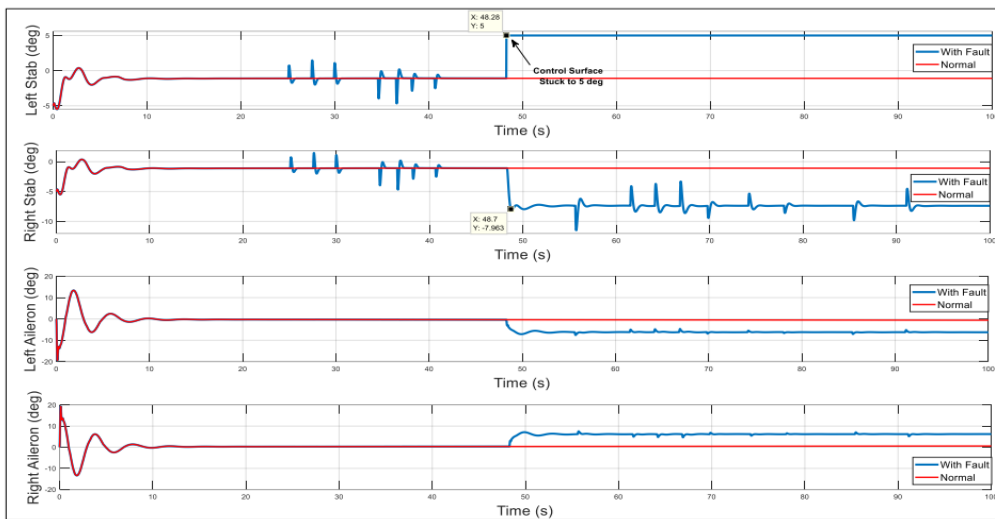


Fig.5: Control surface positions for actuator stuck fault

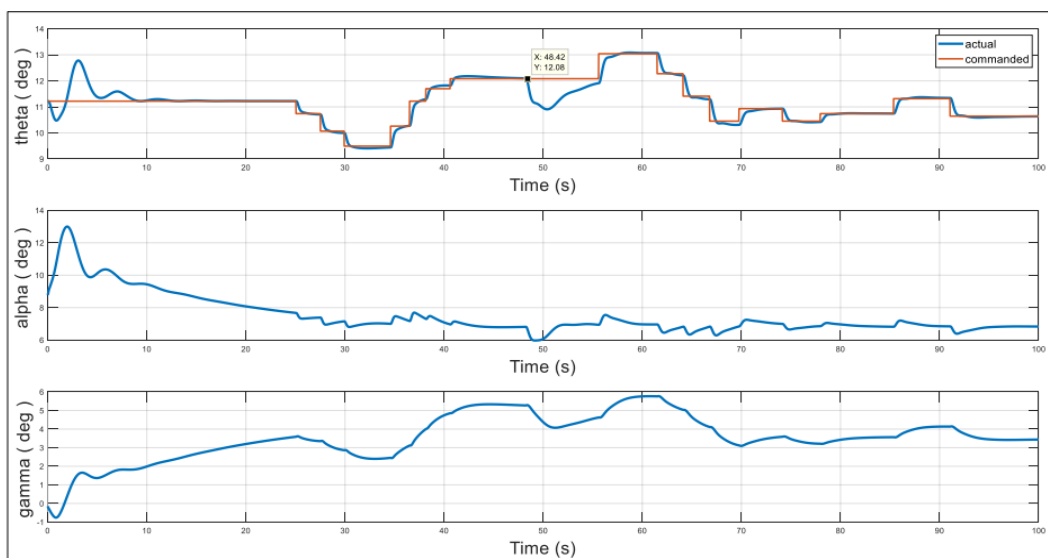
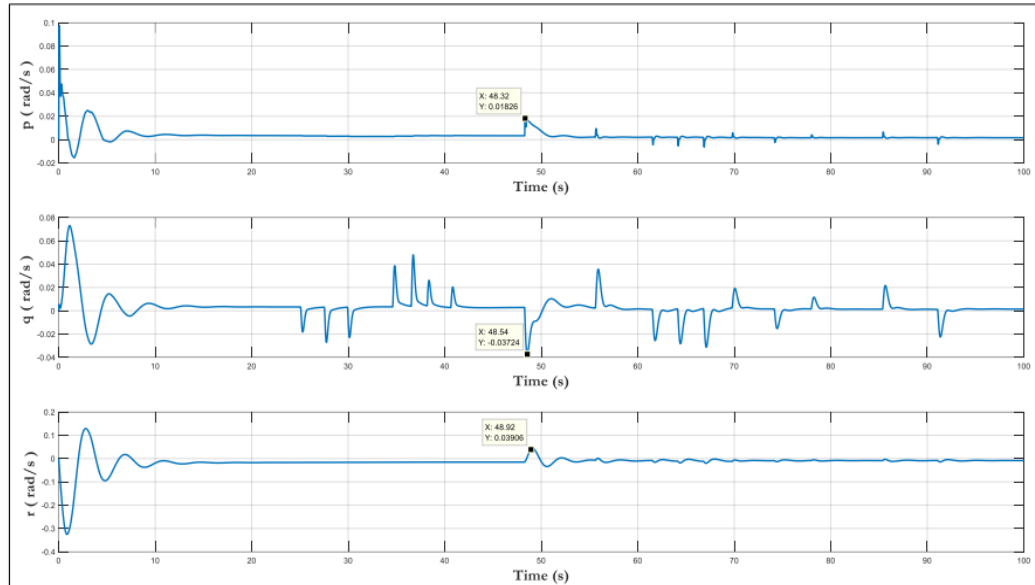


Fig.6: Euler angles for actuator stuck fault



**Fig.7:** Angular rates for actuator stuck fault

## 4.2 Actuator Ineffective Problem

In this case the LSTAB actuator becomes ineffective after 50 sec and floats in air out of aerodynamic forces acting on it resulting in zero net force to aircraft. In this condition also the RSTAB is pushed further down to generate sufficient lift and the ailerons are moved to counter the moment resulting out of asymmetry in stabilizers. The simulation results are shown in figure 7,8 and, 9.

## 4.3 Robustness Analysis

The Robustness of the PID controller is evaluated by using same controller with extended operating point E1, E2, E3 and E4 refer fig. 11.0. The extended operating points are obtained by out-spreading the normal operating point in its neighbourhood. The simulations were carried out with the four extended operating points for LSTAB actuator ineffective case and for and LSTAB actuator stuck case and it was found that the controller is robust enough to follow the commanded inputs with extended operating points also. The figures 12 to 17 shows the case for operating points E1 and E2, where LSTAB becomes ineffective after some duration. Similarly, the figures 18 to 23 represent the controller performance in case of operating points E3 & E4 where LSTAB gets stuck at -5 deg after some duration of levelled flight. In all the cases, the controller was found resilient to change in operating points before and after introduction of fault for different pitch angles. In this condition also the RSTAB is pushed further down to generate sufficient lift and the ailerons are moved to



counter the moment resulting out of asymmetry in stabilizers.

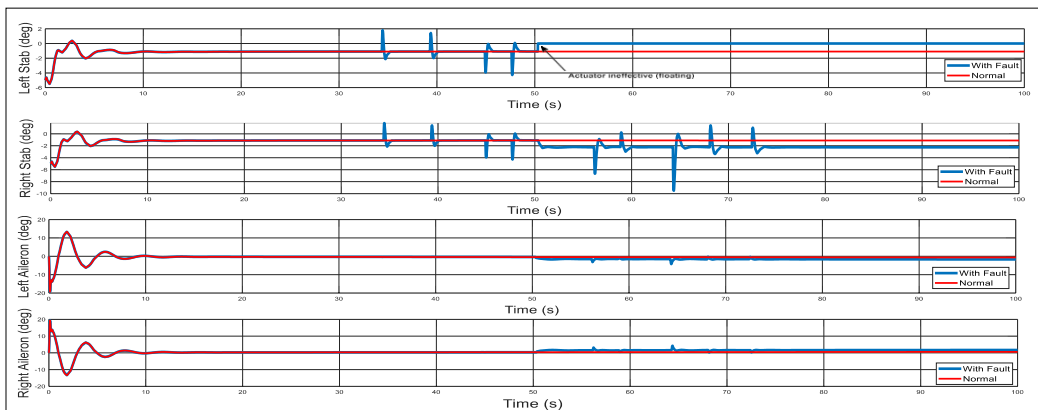


**Fig.8** Control surface positions for ineffective control surface fault

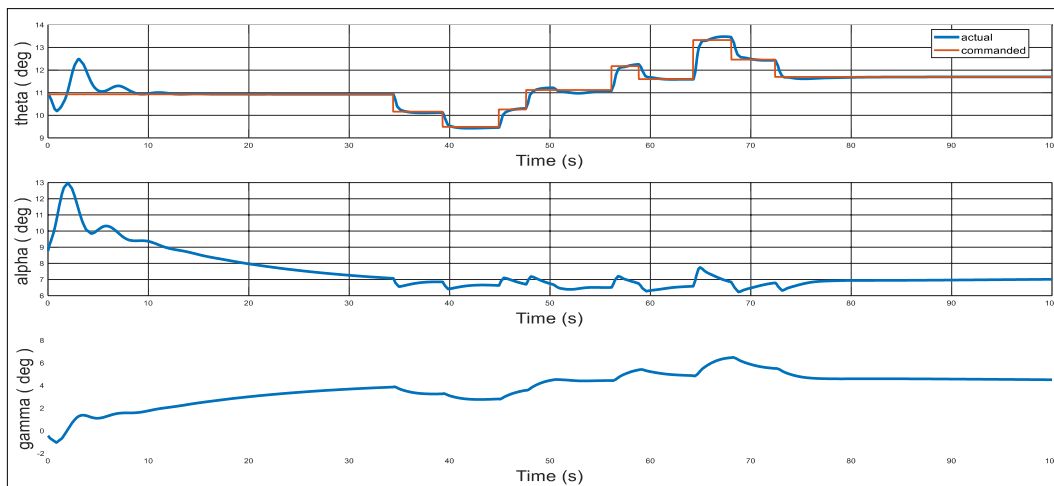


**Fig.9:** Euler angles ineffective control surface fault

### 4.3 Robustness Analysis

The Robustness of the PID controller is evaluated by using same controller with extended operating point E1, E2, E3 and E4 refer fig. 11.0. The extended operating points are obtained by outspreading the normal operating point in its neighbourhood. The simulations were carried out with the four extended operating points for LSTAB actuator ineffective case and for and LSTAB actuator stuck case and it was found that the controller is robust enough to follow the commanded inputs with extended operating points also. The figures 12 to 17 shows the case for operating points E1 and E2, where LSTAB becomes ineffective after some duration. Similarly, the figures 18 to 23 represent the controller performance in



case of operating points E3 & E4 where LSTAB gets stuck at -5 deg after some duration of levelled flight. In all the cases, the controller was found resilient to change in operating points before and after introduction of fault for different pitch angles.

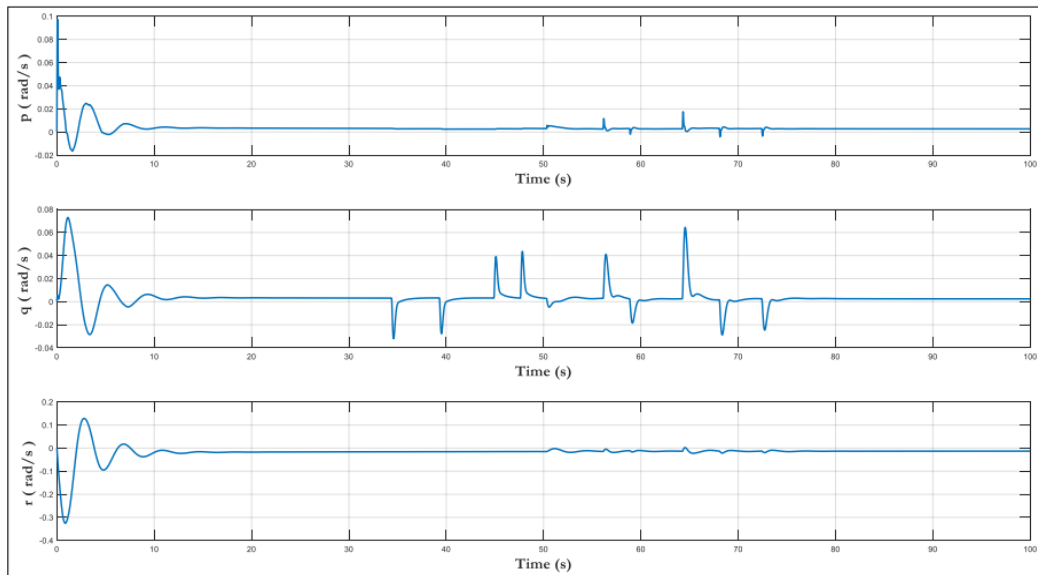


**Fig.10:** Angular rates ineffective control surface fault

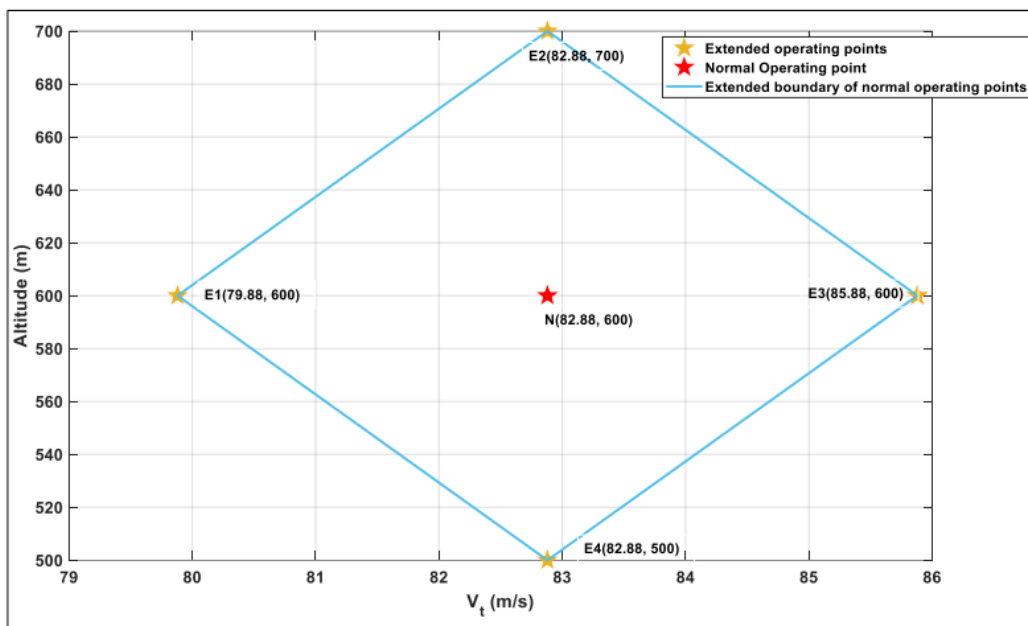


**Fig 11:** Extended operating points in the neighbourhood of nominal operating point

The Fig. 5 to Fig.10 corroborates the ability of controller to follow the given inputs in



presence of actuator lock in place or actuator in floating position. Also, it has been demonstrated that the controller is Robust enough for the change in the extended operating points. This study is based on Proportional Integral and Derivative controllers. It shall be extended further on other different control strategies.

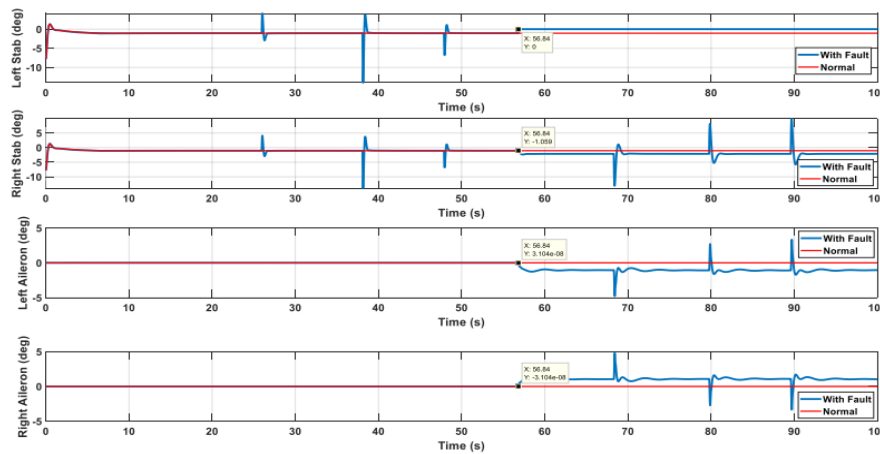


**Fig.12** Control surface positions for extended operating point E1with LSTAB actuator ineffective @ 56.84 seconds

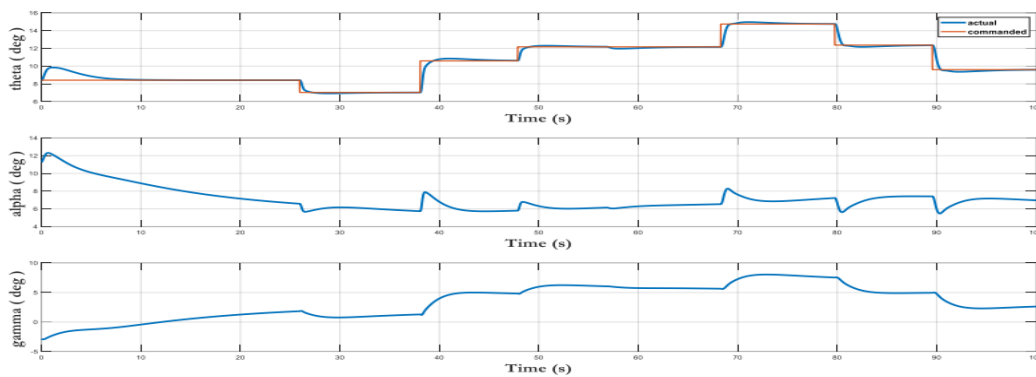


**Fig.13** Euler angles for extended operating point E1with LSTAB actuator ineffective @ 56.84 seconds



Received: 16-01-2024

Revised: 12-02-2024

Accepted: 07-03-2024

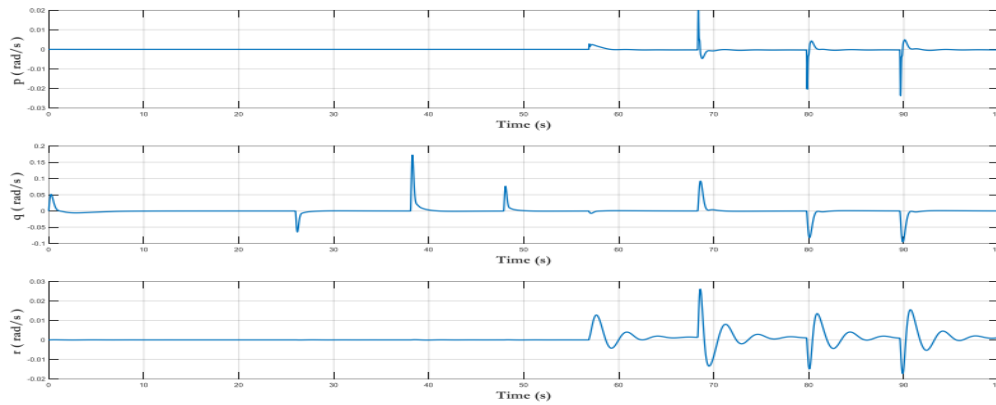


**Fig.14** Angular rates for extended operating point E1 with LSTAB actuator ineffective @ 56.84 seconds

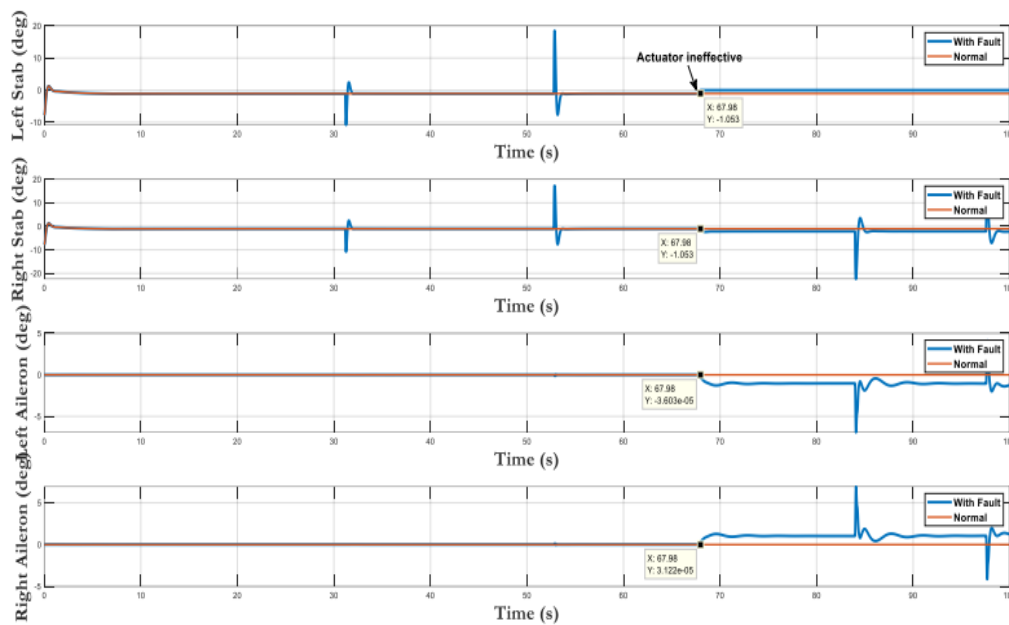


**Fig.15** Control surface positions for extended operating point E2 with LSTAB actuator ineffective @ 67.98 seconds



Received: 16-01-2024

Revised: 12-02-2024

Accepted: 07-03-2024

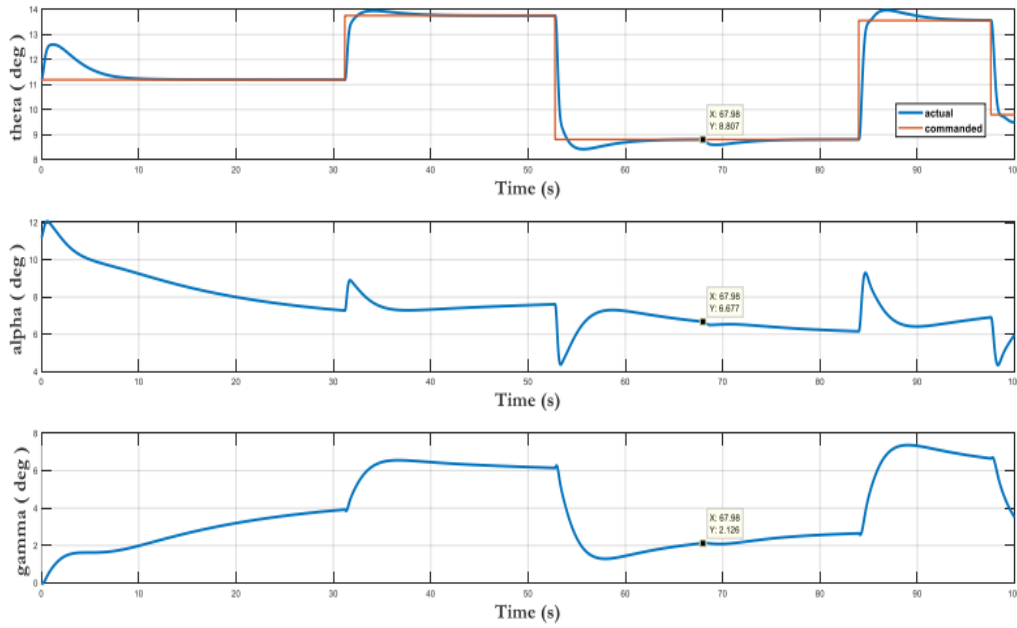


**Fig.16** Euler angles for extended operating point E2 with LSTAB actuator ineffective @ 67.98 seconds

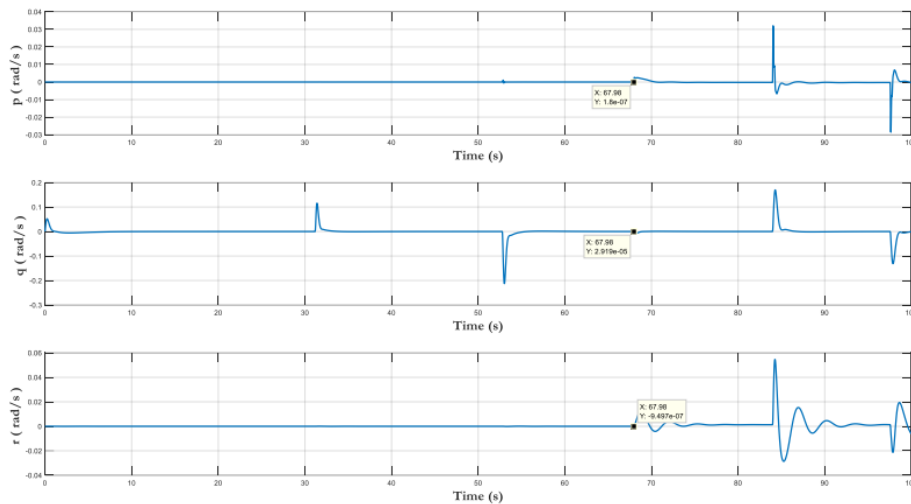


**Fig.17** Angular rates for extended operating point E2 with LSTAB actuator ineffective @ 67.98 seconds



Received: 16-01-2024

Revised: 12-02-2024

Accepted: 07-03-2024

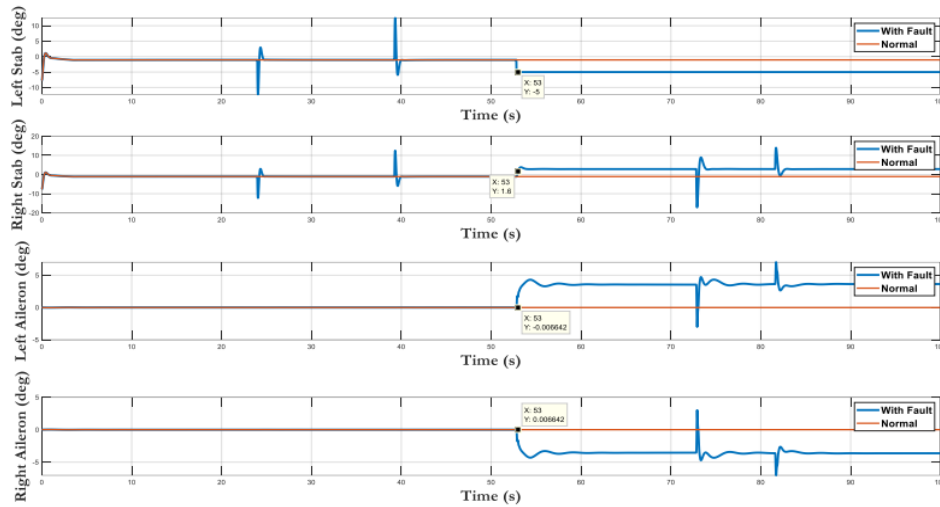


**Fig.18** Control surface positions for extended operating point E3 with LSTAB actuator stuck @ 53 seconds

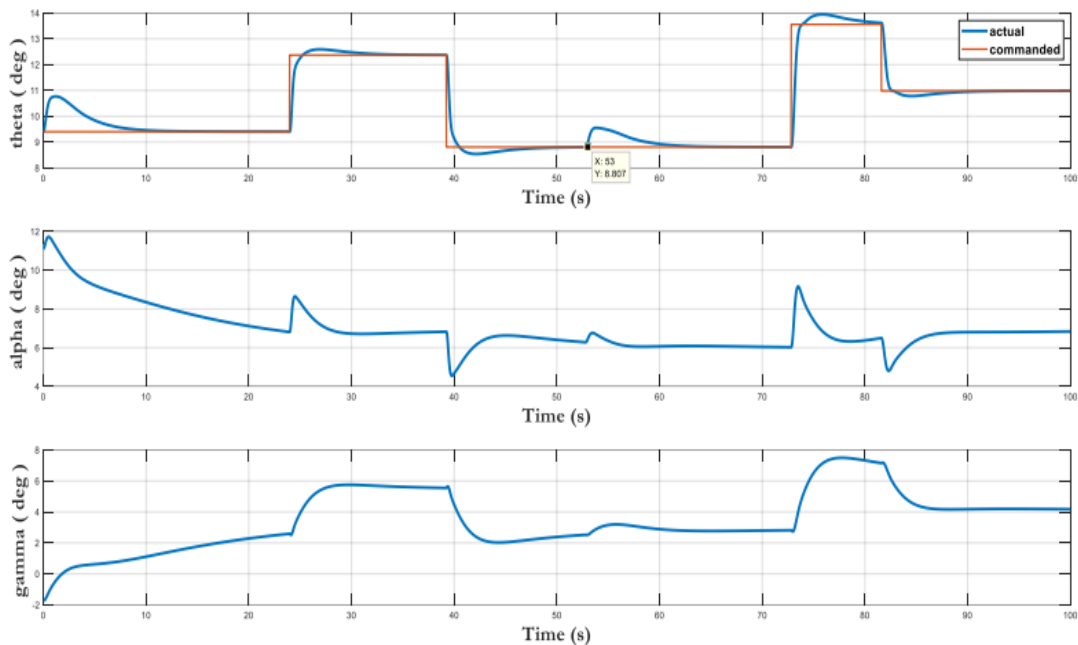


**Fig 19** Euler Angles for extended operating point E3 with LSTAB actuator stuck @ 53 seconds



Received: 16-01-2024

Revised: 12-02-2024

Accepted: 07-03-2024

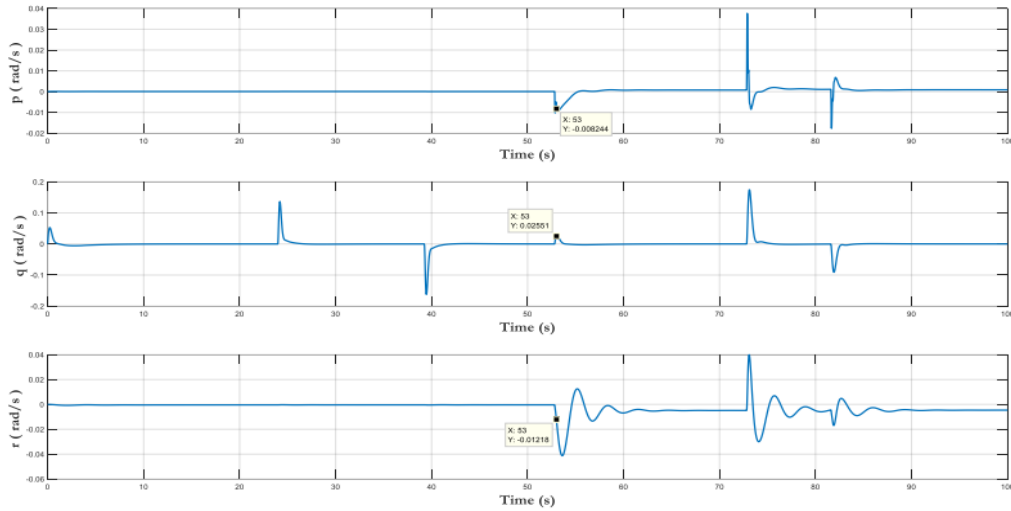


**Fig.20** Angular Rates for extended operating point E3 with LSTAB actuator stuck @ 53 seconds

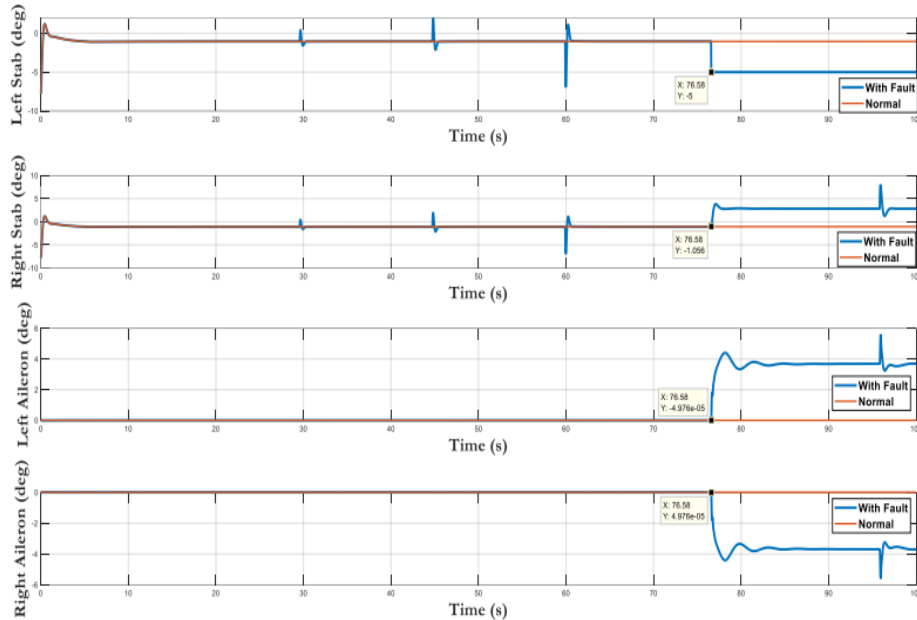


**Fig.21** Control Surface Positions for extended operating point E4 with LSTAB actuator stuck @ 76.58 seconds

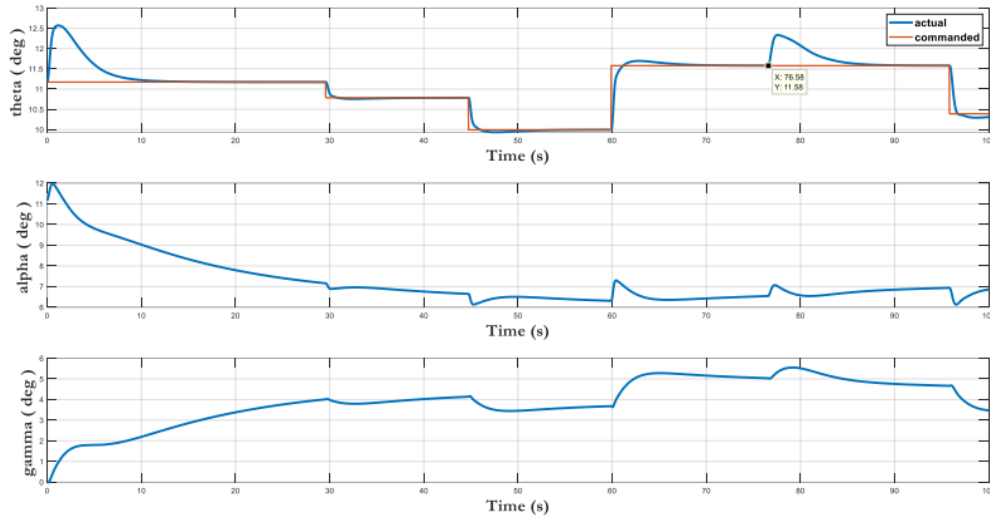


**Fig.22** Euler Angles for extended operating point E4 with LSTAB actuator stuck @ 76.58 seconds

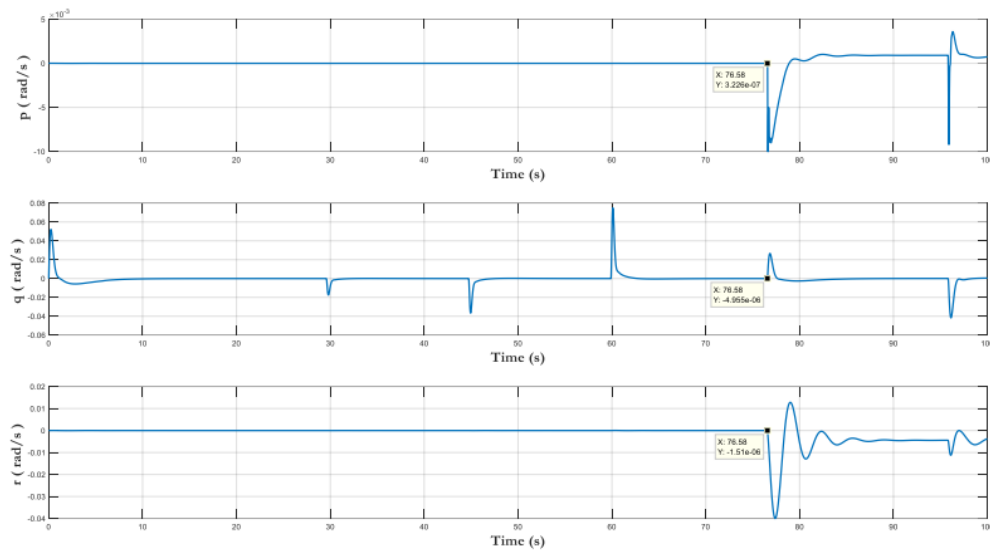


**Fig.23** Angular rates for extended operating point E4 with LSTAB actuator stuck @ 76.58 seconds

## 5. Conclusion

The FDI algorithm is discussed and the capability of the controller for handling actuator stuck (lock in place) and control surface ineffectiveness are shown. The FDI algorithm is



capable to detect the faulty inputs through RM (redundancy manager) which shall also monitor the health of the sensors. Also, the controller is capable to handle the stuck faults and the surface ineffectiveness in a leveled flight.

## References

1. Stengel, R.F. Intelligent failure-tolerant control. *IEEE Control Syst.* 1991, 11, 14–23.
2. Patton, R.J. Fault-tolerant control: The 1997 situation. *IFAC Proc. Vol.* 1997, 30, 1029–1051.
3. Lunze, J.; Richter, J.H. Reconfigurable fault-tolerant control: A tutorial introduction. *Eur. J.Control* 2008, 14, 359.
4. Moor, T. A discussion of fault-tolerant supervisory control in terms of formal languages. *Annu. Rev. Control* 2016, 41, 159–169.
5. Abbaspour, A.; Yen, K.K.; Forouzannezhad, P.; Sargolzaei, A. A Neural Adaptive Approach for Active Fault-tolerant Control Design in UAV. *IEEE Trans. Syst. Man Cybern. Syst.* 2018,50, 3401–3411.
6. Guaranteed Model Based Fault Detection in cyber physical systems: A model Invalidation approach, Farshad Hari, Necmiye Ozay, arXiv:1609.05921, 2017.
7. Development of fault tolerant flight control system for handling actuator stuck fault, *Journal of Aerospace Sciences and Technologies*, V75 N2/1188-2023. 21 Feb 2022.